

DOI: 10.1002/anie.200601264

Exceptionally Strong Electronic Communication through Hydrogen Bonds in Porphyrin–C₆₀ Pairs***Luis Sánchez, Maria Sierra, Nazario Martín,*
Andrew J. Myles, Trevor J. Dale, Julius Rebek, Jr.,*
Wolfgang Seitz, and Dirk M. Guldi***In memory of Roger Taylor*

Proton pumping in the photosynthetic reaction center and conduction of electrons in cytochrome C are significant examples of biological processes governed by supramolecular interactions.^[1] The key function of these examples is electron transfer, which is powered through a network of hydrogen bonds. As a result, hydrogen-bonded donor–acceptor assemblies have emerged as a benchmark for biomimetic model systems: they provide the means for understanding and controlling the role of hydrogen-bonding networks either as a simple molecular interface or, more interestingly, as an actively functioning motif (namely, by assisting more efficient electron-transfer events). These effects largely result from the high efficiency that this supramolecular motif offers in controlling through-bond-mediated electron-transfer processes as well as long-range electronic coupling between donors and acceptors.^[2] Pioneering work carried out by Sessler and

[*] Dr. L. Sánchez, M. Sierra, Prof. Dr. N. Martín
Departamento de Química Orgánica
Facultad de Química
Universidad Complutense de Madrid, 28040 Madrid (Spain)
Fax: (+ 34) 91-394-4103
E-mail: nazmar@quim.ucm.es

Dr. A. J. Myles, T. J. Dale, Prof. Dr. J. Rebek, Jr.
The Skaggs Institute for Chemical Biology and Department of
Chemistry
The Scripps Research Institute
10550 North Torrey Pines Road (MB26), La Jolla, CA 92037 (USA)
Fax: (+ 34) 91-394-4103
E-mail: jrebek@scripps.edu

W. Seitz, Prof. Dr. D. M. Guldi
Institut für Physikalische und Theoretische Chemie
Universität Erlangen-Nürnberg
Egerlandstrasse 3, 91058 Erlangen (Germany)
Fax: (+ 49) 9131-852-830
E-mail: dirk.guldi@chemie.uni-erlangen.de

[**] This work was supported by the MEC of Spain and Comunidad de Madrid (CTQ2005-02609/BTQ and P-PPQ-000225-0505), the Deutsche Forschungsgemeinschaft (SFB 583), FCI, the Office of Basic Energy Sciences of the US Department of Energy (contribution No. NDRL-4670 from the Notre Dame Radiation Laboratory), and the Skaggs Institute for Chemical Biology. M.S. is indebted to MEC of Spain for a PhD fellowship, A.J.M. is a NSERC postdoctoral fellow, and T.J.D. is a Skaggs predoctoral fellow.



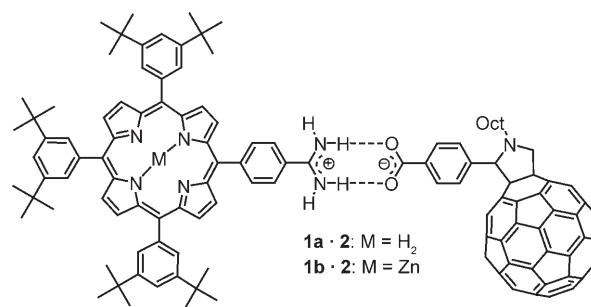
Supporting information for this article is available on the WWW under <http://www.angewandte.org> or from the author.

Therien have demonstrated that the electronic communication through hydrogen-bonding interfaces is more efficient than those found in comparable σ - or π -bonding networks.^[3] Electron-transfer events also impart on the function of artificial devices, such as organic photovoltaics.^[4] The incentives for creating (supra)molecular heterojunctions by, for example, integrating photo-/electroactive donors and acceptors that bear complementary binding sites into functional architectures are 1) facilitation of charge transport and 2) increase in energy conversion efficiency.^[5]

The relevance of fullerenes as spherical electron acceptors in the construction of novel artificial photosynthetic models and in high-performance organic solar cells is incontestable.^[4–6] The combination of the characteristic selectivity and directionality of hydrogen bonds with an efficient electron-transfer process through a noncovalent framework is expected to set new milestones, especially in terms of achieving longer-lived radical-ion-pair states. In fact, a plethora of covalent C_{60} -donor conjugates have stimulated evolutionary advances and revolutionary breakthroughs in the context of converting light into high-energy chemical products or electrical currents.^[7] Very little is, however, known about noncovalent C_{60} -based hybrid ensembles.^[8] To our knowledge, no C_{60} -based examples of electron-transfer processes that occur exclusively through hydrogen-bonded networks have been reported. We present herein a set of noncovalently associated C_{60} -porphyrin ensembles (**1–2**) interfaced by a two-point amidinium–carboxylate pair that facilitates an efficient charge-separation process to afford microsecond-lived $P^{+}-C_{60}^{-}$ radical pairs. The latter is particularly stable, even in highly polar solvents, as a result of the synergy of hydrogen bonds and electrostatic interactions.^[9] Beneficial effects also materialize from other salt pairs, that is, guanidinium–carboxylate, especially in terms of structural aspects.^[10] Notably, the noncovalent binding motif utilized herein, amidinium–carboxylate, diminishes the possible bonding modes and, therefore, favors the linearity of the final interfaced pair. In addition, the rational design, that is, placing the amidinium and carboxylate functionalities at the porphyrins and C_{60} , respectively, reinforces the strength of the hydrogen-bonding network and ensures an optimal pathway for the motion of charges and the electronic coupling between both electroactive units.^[9a]

The synthesis of the new **1–2** ensembles started from a previously reported porphyrin amidine donor **1a, b**^[11] and fulleropyrrolidine carboxylic acid **2**.^[12] Directly mixing both components readily yields target ensembles, namely, noncovalently bonded hybrids **1–2** (see Scheme 1 and the Supporting Information).

Complex formation between **1a** and **2** was monitored by ¹H NMR spectroscopy (3 mM, [D₈]THF). Upon titration of one equivalent of **2** into a solution of **1a**, a series of resonance shifts are observed (Figure 1). The most dramatic shift involves the aryl protons *ortho* to the amidine functionality ($\Delta\delta = 0.35$ ppm).^[13] Although the amidine protons are not resolved in the ¹H NMR spectrum of **1a**, formation of **1a–2** resolves two broad downfield resonances at $\delta = 9.4$ and 13.1 ppm. These new peaks each integrate for two protons and are attributed to the two different amidine protons.



Scheme 1. Amidinium–carboxylate interfaced porphyrin– C_{60} assemblies (**1–2**).

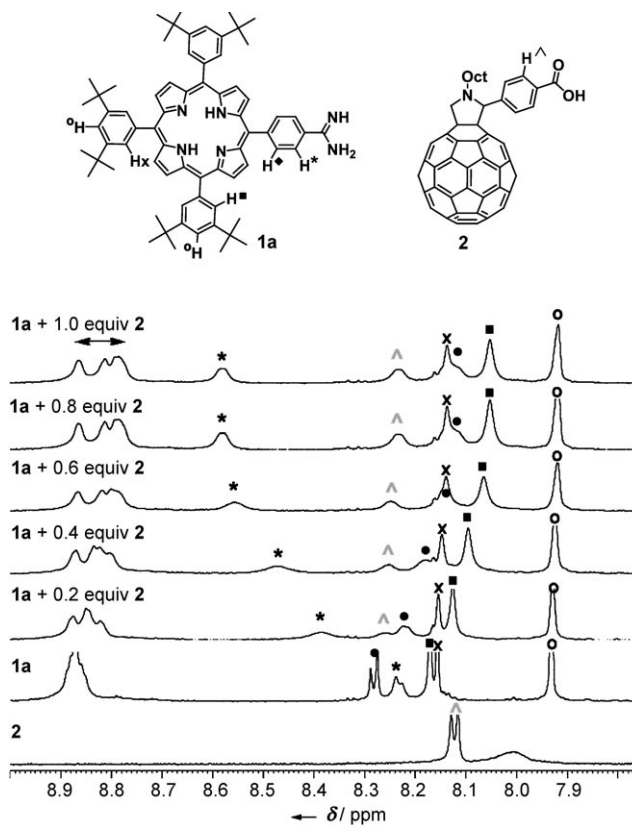


Figure 1. ¹H NMR shifts upon titration of **2** into a solution of **1a** in [D₈]THF.

Importantly, no further changes are observed upon addition of more than one equivalent of **2**, thus confirming the exclusive presence of a strong 1:1 complex.^[14]

Further details on the formation of **1a–2** and **1b–2** were obtained from experiments in which dilute solutions of **1a** and **1b** in toluene/acetonitrile (9:1, v/v) or THF were titrated with variable amounts of **2** and probed by absorption and fluorescence spectroscopy (see Figure 2 and the Supporting Information in which a typical example for an absorption measurement is given). Relative to the component spectra (**1b** and **2**), a number of differences are apparent. For **1b**, Soret- and Q-band transitions at 428 and 558 nm, respectively, shift incrementally to the red (431 and 560 nm). Moreover, the presence of isosbestic points indicate the transformation

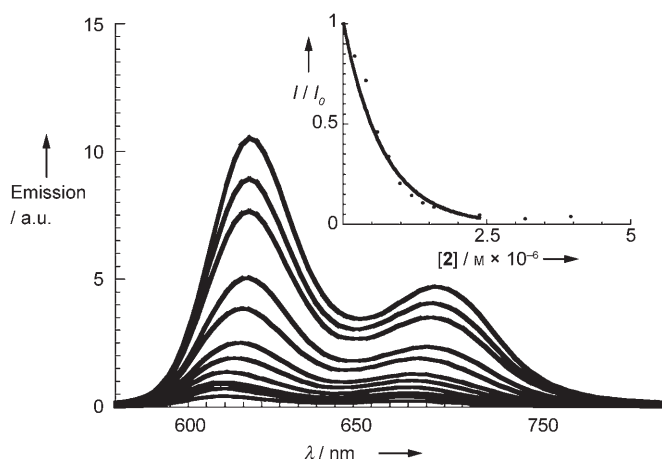


Figure 2. Fluorescence spectra ($\lambda_{\text{exc}} = 433 \text{ nm}$) of **1b** ($1.08 \times 10^{-6} \text{ M}$) and variable concentration of **2** (0, 0.2, 0.4, 0.6, 0.8, 1.0, 1.2, 1.4, 1.6, 2.4, 3.9, 9.1, and $23.7 \times 10^{-6} \text{ M}$) in toluene/acetonitrile (9:1, v/v) at room temperature. Insert displays the relationship of I/I_0 versus $[2]$ that was used to determine the association constant. I = current intensity in relative units.

of **1b** (the starting point of the titration) into **1b·2** (the end point of the titration). The changes in absorption were further employed to confirm the stoichiometry of **1a·2** and **1b·2** through Job plots. In this light, Gaussian relationships with maxima at 0.5 unequivocally confirm the 1:1 complex stoichiometries that were evoked from the ^1H NMR experiments (see the Supporting Information).

In excitation experiments with **1a** and **1b**, strong fluorescence emissions are seen in the red region, with quantum yields of 0.2 and 0.04, respectively. When variable concentrations of **2** are present, the fluorescence emission intensities decreased exponentially (see Figure 2 and the Supporting Information). Nonlinear least-square analyses, that is, fluorescence intensity versus concentration of **2**, allowed the evaluation of the binding constants of **1·2**, which are exceptionally high. In solvents that do not interfere significantly with either the electrostatic or the hydrogen-bonding interactions (toluene or toluene/acetonitrile (9:1, v/v)), binding constants as high as $2.1 \times 10^7 \text{ M}^{-1}$ were deduced. The binding constants in THF, in which interactions are mostly based on electrostatic attractions, showed values between $1.3 \times 10^5 \text{ M}^{-1}$ (**1a·2**) and $3.3 \times 10^5 \text{ M}^{-1}$ (**1b·2**).

Potential C_{60} interactions with **1a** or **1b** were tested in a series of reference assays. For example, in the absence of the amidine and carboxylic acid functionalities, the absorption spectra remain virtually as the superimpositions of the component spectra throughout the titrations. The lack of mutually interacting systems was also confirmed in fluorescence experiments. Overall, only a quenching of less than 5% is noted, relative to > 95% quenching in **1a·2** or **1b·2**.

The redox features of interfaced **1·2** pairs were determined by cyclic voltammetry in THF at room temperature (see the Supporting Information). These values provide useful information about the energies of the radical ion pairs formed upon photoexcitation (see below). The cyclic voltammograms of both porphyrins, free base (**1a**) and zinc (**1b**) at concentrations of $5 \times 10^{-4} \text{ M}$, show sets of reversible

reduction and oxidation steps (Figure 3). For **2**, three reduction steps are discernable. The corresponding zinc complex **1b·2** reveals cathodic shifts of the reduction and oxidation steps relative to the free-base complex **1a·2** (see the Supporting Information). In both **1·2** complexes, the redox patterns of the two constituents, namely porphyrin amidines **1** and C_{60} carboxylic acid **2**, are essentially preserved (Figure 3).

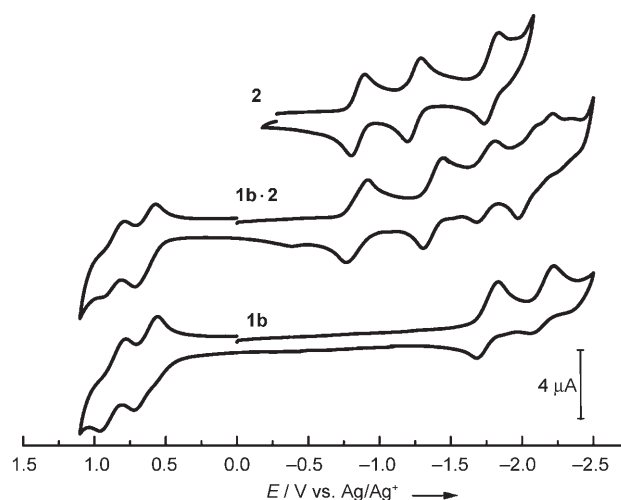


Figure 3. Cyclic voltammograms of **1b·2** and its precursors **1b** and **2**, measured in THF ($5 \times 10^{-4} \text{ M}$) at 100 mVs^{-1} (V vs. Ag/Ag^+).

The observed slight shifts in the redox potentials of the **1·2** assemblies could be accounted for by a pronounced electronic coupling between both electroactive components (see below). Neglecting significant electronic interactions, we estimate values of the radical-ion-pair-state energies as the sum of the first reduction potential of **2** and the first oxidation potential of either **1a** or **1b** to be 1.9 and 1.62 eV for **1a·2** and **1b·2**, respectively. In other words, radical-ion-pair formations that evolve from the singlet excited states are highly exothermic.

Finally, transient absorption studies showed the fate of the porphyrin excited states and the identification of the photo-products. Pumping light into the ground state of **1a** or **1b** with short 387-nm (namely, 150 fs) or 532-nm (namely, 6 ns) laser pulses led to the population of their singlet excited states. The latter undergo intersystem crossing ($\approx 10^8 \text{ s}^{-1}$) to the long-lived and molecular-oxygen-sensitive triplet states. Triplet spectra of **1a** or **1b** reveal, besides bleaching in the Soret- and Q-band region, characteristic triplet maxima at 780 (**1a**) or 840 nm (**1b**).^[6d]

Initially, the porphyrin chromophores in **1a·2** and **1b·2** produce notable singlet fingerprints for **1a** and **1b** upon photoexcitation. This behavior attests to the successful excitation of **1a** and **1b**. However, instead of the slow intersystem crossings, the singlet excited states decay with rates of about 10^{10} s^{-1} , from which we deduce an electronic coupling of 36 cm^{-1} between both electroactive elements (that is, **1b·2**). At the end of the intrinsically fast decay, differential absorption changes in the visible region are governed by broad absorptions at 600–800 nm, thus indicating **1a**- or **1b**-centered oxidation products. In the near-infrared region, on the other hand, the signature of a **2**-centered

reduction is seen at 1000 nm.^[15] Figure 4 exemplifies the spectral changes seen in the cases of **1b-2** and **1a-2**, respectively (see the Supporting Information also). The decay kinetics of both signatures—on the nanosecond

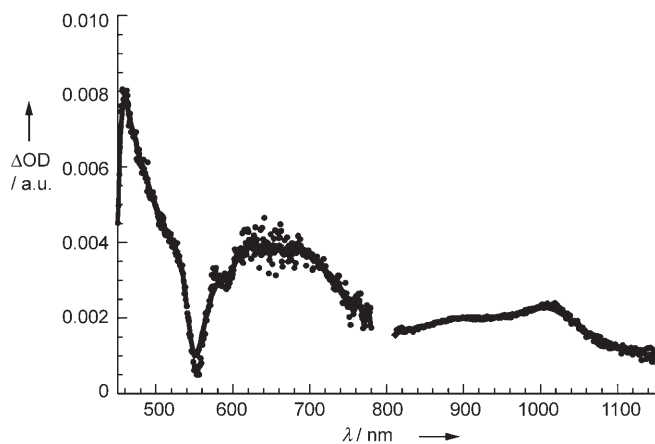


Figure 4. Transient absorption spectrum (NIR part) of **1b-2** in toluene at room temperature recorded 50 ps following a 150 fs laser pulse ($\lambda_{\text{exc}} = 387 \text{ nm}$).

scale—reflect the return of the radical-ion-pair states to the electronic ground states. The lifetime of the newly formed radical-ion-pair state, as derived by analyzing several wavelengths under unimolecular conditions, are 9.3 ± 0.1 and $7.9 \pm 0.5 \mu\text{s}$ for **1a-2** and **1b-2**, respectively, in THF (see the Supporting Information).

In summary, the two-point amidinium–carboxylate binding motif guarantees an extraordinary stabilization for a set of noncovalently interfaced ensembles (**1-2**). Association constants reach up to 10^7 M^{-1} . Exceptionally strong electronic couplings stem from such binding, which in turn facilitate a faster, more efficient, and longer-lived formation of radical-ion-pair states (that is, $\approx 10 \mu\text{s}$ in THF) relative to similar covalent C_{60} conjugates (namely, $\approx 1 \mu\text{s}$ in THF).^[15] Most importantly, such remarkable radical-ion-pair lifetimes outperform previously reported ensembles based on 1) a non-amidinium–carboxylate binding motif^[8] or 2) non-fullerene electron acceptors^[2,9] by several orders of magnitude. These results point unmistakably to the fundamental advantages of strong and highly directional hydrogen-bonding networks in assisting electron-transfer processes and pave the way to the construction of efficient photovoltaic devices inspired by biomimetic principles.

Received: March 31, 2006
Published online: June 22, 2006

Keywords: electron transfer · electronic coupling · fullerenes · hydrogen bond

- [1] a) J. A. Stubbe, D. G. Nocera, C. S. Yee, M. C. Y. Chang, *Chem. Rev.* **2003**, *103*, 2167–2201; b) A. Namslauer, A. Aagaard, A. Katsonouri, P. Brzezinski, *Biochemistry* **2003**, *42*, 1488–1498.
[2] a) A. P. H. J. Schenning, J. V. Herrikhuyzen, P. Jonkheijm, Z. Chen, F. Würthner, E. W. Meijer, *J. Am. Chem. Soc.* **2002**, *124*,

10252–10253; b) J. L. Sessler, M. Sathiosatham, C. T. Brown, T. A. Rhodes, G. Wiederrecht, *J. Am. Chem. Soc.* **2001**, *123*, 3655–3660; c) A. J. Myles, N. R. Branda, *J. Am. Chem. Soc.* **2001**, *123*, 177–178; d) R. K. Castellano, S. L. Craig, C. Nuckolls, J. Rebek, Jr., *J. Am. Chem. Soc.* **2000**, *122*, 7876–7882; e) T. H. Ghaddar, E. W. Castner, S. S. Isied, *J. Am. Chem. Soc.* **2000**, *122*, 1233–1234.

- [3] a) J. L. Sessler, B. Wang, A. Harriman, *J. Am. Chem. Soc.* **1993**, *115*, 10418–10419; b) P. J. F. De Rege, S. A. Williams, M. J. Therien, *Science* **1995**, *269*, 1409–1413.
[4] a) W. Ma, C. Yang, X. Gong, K. Lee, A. J. Heeger, *Adv. Funct. Mater.* **2005**, *15*, 1617–1622; b) G. Li, V. Shrotriya, J. Huang, Y. Yao, T. Moriarty, K. Emery, Y. Yang, *Nat. Mater.* **2005**, *4*, 864–868; c) I. Riedel, E. von Hauff, J. Parisi, N. Martín, F. Giacalone, V. Dyakonov, *Adv. Funct. Mater.* **2005**, *15*, 1979–1987; d) M. W. Wienk, J. M. Kroon, W. J. H. Verhees, J. Knol, J. C. Hummelen, P. A. van Hal, R. A. J. Janssen, *Angew. Chem.* **2003**, *115*, 3493–3497; *Angew. Chem. Int. Ed.* **2003**, *42*, 3371–3375; e) C. J. Brabec, N. S. Sariciftci, J. C. Hummelen, *Adv. Funct. Mater.* **2001**, *11*, 15–26.
[5] a) C.-H. Huang, N. D. McClenaghan, A. Kuhn, J. W. Hofstraat, D. M. Bassani, *Org. Lett.* **2005**, *7*, 3409–3412; b) J. L. Brédas, D. Beljonne, V. Coropceanu, J. Cornil, *Chem. Rev.* **2004**, *104*, 4971–5003; c) M. A. Fox, *Acc. Chem. Res.* **1999**, *32*, 201–207.
[6] a) H. Imahori, Y. Sakata, *Adv. Mater.* **1997**, *9*, 537–546; b) N. Martín, L. Sánchez, B. Illescas, I. Pérez, *Chem. Rev.* **1998**, *98*, 2527–2548; c) D. M. Guldi, N. Martín, *J. Mater. Chem.* **2002**, *12*, 1978–1992; d) D. M. Guldi, *Chem. Soc. Rev.* **2002**, *31*, 22–36; e) J.-F. Nierengarten, *Top. Curr. Chem.* **2003**, *228*, 87–110; f) J. L. Segura, N. Martín, D. M. Guldi, *Chem. Soc. Rev.* **2005**, *34*, 31–47; g) D. M. Guldi, G. M. A. Rahman, C. Ehli, V. Sgobba, *Chem. Soc. Rev.* **2006**, *35*, 471–487.
[7] For recent examples, see: a) C. M. Atienza, G. Fernández, L. Sánchez, N. Martín, I. Sá Dantas, M. W. Wienk, R. A. J. Janssen, G. M. A. Rahman, D. M. Guldi, *Chem. Commun.* **2006**, 514–516; b) G. Kodis, Y. Terazono, P. A. Liddell, J. Andréasson, V. Garg, M. Hamburger, T. A. Moore, A. L. Moore, D. Gust, *J. Am. Chem. Soc.* **2006**, *128*, 1818–1827; c) L. Sánchez, M. Sierra, N. Martín, D. M. Guldi, M. W. Wienk, R. A. J. Janssen, *Org. Lett.* **2005**, *7*, 1691–1694; d) T. Oike, T. Kurata, K. Takimiya, T. Otsubo, Y. Aso, H. Zhang, Y. Araki, O. Ito, *J. Am. Chem. Soc.* **2005**, *127*, 15372–15373; e) D. M. Guldi, F. Giacalone, G. de la Torre, J. L. Segura, N. Martín, *Chem. Eur. J.* **2005**, *11*, 7199–7210; f) L. Sánchez, M. A. Herranz, N. Martín *J. Mater. Chem.* **2005**, *15*, 1409–1421; g) R. S. Iglesias, C. G. Claessens, T. Torres, G. M. A. Rahman, D. M. Guldi, *Chem. Commun.* **2005**, 2113–2115; h) K. Ohkubo, H. Kotani, J. Shao, Z. Ou, K. M. Kadish, G. Li, R. K. Pandey, M. Fujitsuka, O. Ito, H. Imahori, S. Fukuzumi, *Angew. Chem.* **2004**, *116*, 871–874; *Angew. Chem. Int. Ed.* **2004**, *43*, 853–856; i) F. Giacalone, J. L. Segura, N. Martín, D. M. Guldi, *J. Am. Chem. Soc.* **2004**, *126*, 5340–5341; j) M. Gutierrez-Nava, G. Accorsi, P. Masson, N. Armaroli, J. F. Nierengarten, *Chem. Eur. J.* **2004**, *10*, 5076–5086.
[8] a) F. Diederich, M. Gómez-López, *Chem. Soc. Rev.* **1999**, *28*, 263–278; b) L. Sánchez, N. Martín, D. M. Guldi, *Angew. Chem.* **2005**, *117*, 5508–5516; *Angew. Chem. Int. Ed.* **2005**, *44*, 5374–5382; c) *Special Issue on Supramolecular Chemistry of Fullerenes* (Eds.: N. Martín, J. F. Nierengarten), *Tetrahedron* **2006**, *62*, 1905–2132; d) U. Hahn, M. Elhabiri, A. Trabolsi, H. Herschbach, E. Leize, A. Van Dorsselaer, A.-M. Albrecht-Gary, J.-F. Nierengarten, *Angew. Chem.* **2005**, *117*, 5472–5475; *Angew. Chem. Int. Ed.* **2005**, *44*, 5338–5341; e) N. D. McClenaghan, Z. Grote, K. Darriet, M. Zimine, R. M. Williams, L. De Cola, D. M. Bassani, *Org. Lett.* **2005**, *7*, 807–810; f) J. L. Sessler, J. Jayawickramarajah, A. Gouloumis, T. Torres, D. M. Guldi, S. Maldonado, K. J. Stevenson, *Chem. Commun.* **2005**, 1892–1894.

- [9] a) J. P. Kirby, J. A. Roberts, D. G. Nocera, *J. Am. Chem. Soc.* **1997**, *119*, 9230–9236; b) N. H. Damrauer, J. M. Hodgkiss, J. Rosenthal, D. G. Nocera, *J. Phys. Chem. B* **2004**, *108*, 6315–6321.
- [10] a) M. Haj-Zaroubi, N. W. Mitzel, F. P. Schmidtchen, *Angew. Chem.* **2002**, *114*, 111–114; *Angew. Chem. Int. Ed.* **2002**, *41*, 104–107; b) V. Král, F. P. Schmidtchen, K. Lang, M. Berger, *Org. Lett.* **2002**, *4*, 51–54; c) M. Berger, F. P. Schmidtchen, *Angew. Chem.* **1998**, *110*, 2840–2842; *Angew. Chem. Int. Ed.* **1998**, *37*, 2694–2694.
- [11] J. Otsuki, K. Iwasaki, Y. Nakano, M. Itou, Y. Araki, O. Ito, *Chem. Eur. J.* **2004**, *10*, 3461–3466.
- [12] M. Segura, L. Sánchez, J. de Mendoza, N. Martín, D. M. Guldi, *J. Am. Chem. Soc.* **2003**, *125*, 15093–15100.
- [13] 2D ROESY spectrometry was performed to confirm peak assignments in the 1D ¹H NMR spectrum of **1a**.
- [14] The high stability of the **1a**·**2** complex prevents reliable determination of the association constants using NMR techniques; see Ref. [9].
- [15] H. Imahori, H. Yamada, D. M. Guldi, Y. Endo, A. Shimomura, S. Kundu, K. Yamada, T. Okada, Y. Sakata, S. Fukuzumi, *Angew. Chem.* **2002**, *114*, 2450–2453; *Angew. Chem. Int. Ed.* **2002**, *41*, 2344–2347.